Chemie der Erde 77 (2017) 387–398

Contents lists available at ScienceDirect

Chemie der Erde

journal homepage: www.elsevier.de/chemer

Gold mineralizing efficiency during hydrothermal alteration of the Mesozoic granitoids in the northwest Jiaodong Peninsula: Contrasting conditions between the Guojialing and Linglong plutons

Wen-Gang Xu[a,b], Hong-Rui Fan[a,c,*], Kui-Feng Yang[a,c], Fang-Fang Hu[a,c], Ya-Chun Cai[a]

[a] Key Laboratory of Mineral Resources, Institute of Geology and Geophysics, Chinese Academy of Sciences, Beijing 100029, China
[b] PowerChina Huadong Engineering Corporation Limited, Hangzhou, Zhejiang 311122, China
[c] College of Earth Science, University of Chinese Academy of Sciences, Beijing 100049, China

ARTICLE INFO

Article history:
Received 22 December 2016
Received in revised form 22 June 2017
Accepted 3 August 2017
Editorial handling - Juraj Majzlan

Keywords:
Hydrothermal alteration
Gold mineralizing efficiency
GEM-Selektor
Linglong granite
Guojialing granodiorite
Jiaodong Peninsula
North China Craton

ABSTRACT

Mesozoic granitoids were extensively altered by hydrothermal fluids in the northwest Jiaodong Peninsula, and gold precipitated from the fluids developing prevalent mineralization in this district. The 160–158 Ma Linglong granite and 130–120 Ma Guojialing granodiorite are the major Mesozoic granitoids in this district, both of which are hydrothermally altered and intimately associated with gold mineralization. Although numerous studies were carried out by previous researchers, mainly focusing on tectonics, lithology, mineralogy, geochronology, and fluid geochemistry, knowledge about hydrothermal alteration processes of these granitoids and their gold mineralization efficiency (i.e. which one is more effective to precipitate the gold from its parent solution) is far beyond clear illumination. Geochemical simulation software GEM-Selektor (based on the Gibbs energy minimization algorithm) was applied in this study, which aims to test the gold mineralization efficiency of these two granitoids during the hydrothermal alteration processes. Simulation results indicate that solutions in equilibrium with the Linglong granite are capable of hosting more sulfur than that with the Guojialing granodiorite, since the latter contains more Fe. However, the solutions with these two granitoids display similar gold solubility. "Bulk cooling" simulation results show that the gold mineralization pattern is similar between the Linglong and Guojialing case; "Rock titration" simulation results reveal that the Guojialing granodiorite is prone to precipitate gold more strongly than the Linglong granite, as gold-bearing solutions (or ore-forming fluids) flowing-through at high temperature, equivalent to a deeper level, implying that if the gold mineralization is developed at depth, the Guojialing rock will precipitate more gold. If the gold-bearing solution flow-through the wall rocks relatively fast, and gold mineralization fails to take place, then the Guojialing granodiorite is probably unfavorable for subsequent gold enrichment of the ore-forming fluid. The Linglong granite will precipitate the gold more efficiently from its parent solution at low temperature or at a shallower level, and this is consistent with previous mining prospecting results. Therefore, we suggest that the Guojialing granodiorite should be treated as the main target during future deep prospecting project.

1. Introduction

Hydrothermal alteration is extensively developed in gold deposits in the Jiaodong district, and the mineralization type is called "Jiaojia-type" (e.g. Li et al., 2015; Wen et al., 2015). The wall-rocks altered by ore-forming fluid are mostly Mesozoic granitoids, especially the Linglong granite and Guojialing granodiorite, and gold deposits are frequently hosted by these rocks. Thus, it is widely believed that the hydrothermal alteration processes of these granites are related to gold mineralization (Fan et al., 2003; Chen et al., 2005; Song et al., 2012; Li et al., 2013; Li et al., 2015; Song et al., 2015a; Fan et al., 2016; Jiang et al., 2016; Yang et al., 2016).

The mineral assemblages developed by hydrothermal alteration are generally uniform, mainly consisting of K-feldspar + quartz + sericite + sulfides ± carbonate ± chlorite ± epidote ± magnetite, in which sulfides consist mostly of pyrite with minor pyrrhotite, chalcopyrite, sphalerite, and galena (Li et al., 2015). Besides, hydrothermal alteration stages are also similar for these deposits,

Abbreviations: Bi, biotite; Cal, calcite; Kfs, K-feldspar; Mt, magnetite; Pl, plagioclase; Py, pyrite; Qz, quartz; Sd, siderite; Ser, sericite.

* Corresponding author at: Key Laboratory of Mineral Resources, Institute of Geology and Geophysics, Chinese Academy of Sciences, Beijing 100029, China.
E-mail address: fanhr@mail.iggcas.ac.cn (H.-R. Fan).

http://dx.doi.org/10.1016/j.chemer.2017.08.001
0009-2819/

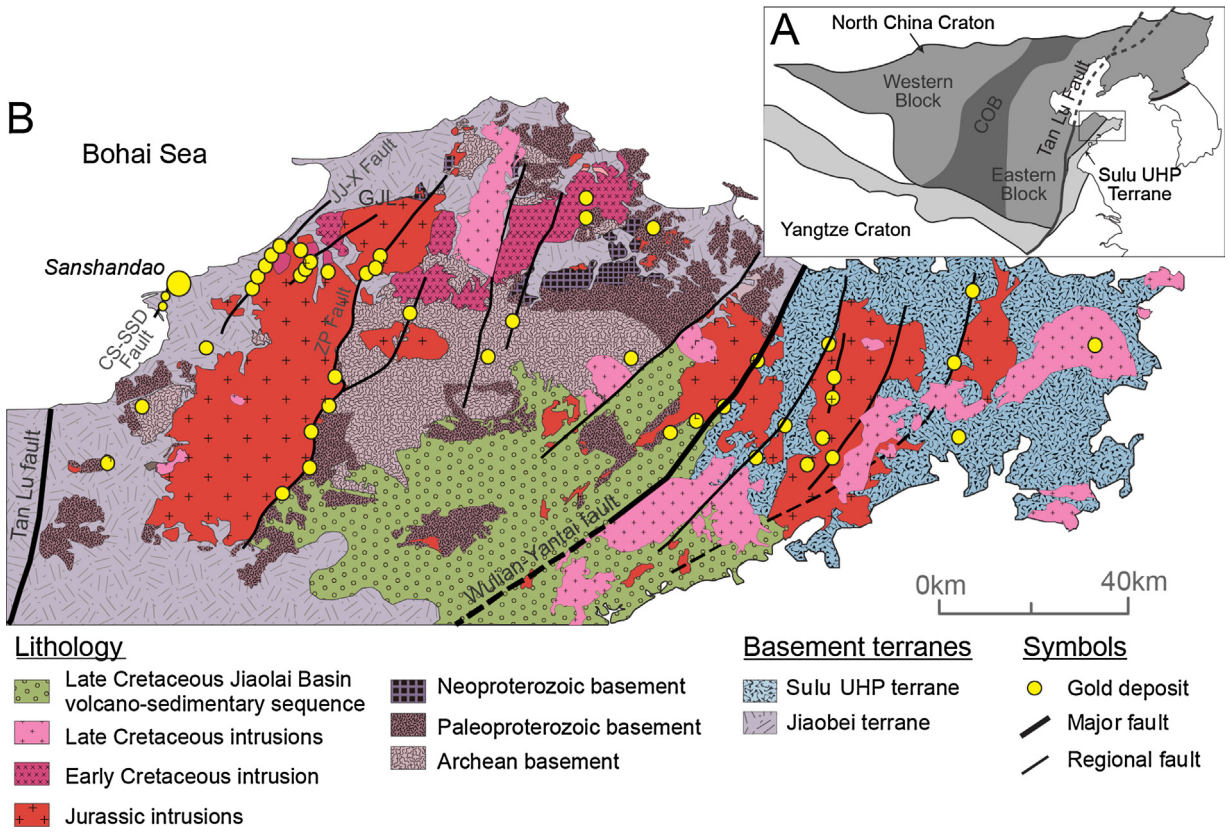

Fig 1. (A) Regional map of the North China Craton, and (B) geological map of the Jiaodong Peninsula (Modified from Fan et al., 2003).

including early potassic alteration + silicification + sericitization-sulfidation (pyritization) + latest carbonatization. These phenomena indicate that the fluids inducing the hydrothermal alterations associated with gold mineralization are consistent for these gold deposits. Although the characteristics of the hydrothermal alteration of these granitic wall rocks are almost identical, the extent of gold mineralization scales varies in different granitoids. For instance, in the Sanshandao gold deposit, the largest one in China with an Au reserve >2000 t (Song et al., 2015b), gold is mainly hosted by the Linglong granite at a shallow level, whereas it changes to be hosted in the Guojialing granodiorite in the deeper sections (Fan et al., 2003, 2016; Jiang et al., 2011; Song et al., 2012; Li et al., 2013). The Jiaojia gold deposit, another large one in northwestern Jiaodong Peninsula, is predominantly hosted by the Linglong granite (Jiang, 2011), but as revealed by a new exploration effort, gold mineralization is also developed in the Guojialing granodiorite located at depth (Prospecting reports). As the exploration goes deeper, the Guojialing granodiorite is increasingly the focus of mining companies. In summary, the gold mineralization capacity of the Linglong and Guojialing intrusions is distinguishable, or, in other words, their gold mineralization efficiency is different.

In this work, we attempt to illuminate the details of the gold mineralization during hydrothermal alteration of the wallrocks of the Linglong and Guojialing intrusions and to interpret the differences of the gold mineralization efficiency between them, providing information for further prospecting projects in this area.

2. Geologic settings

The Jiaodong Peninsula in the eastern part of the North China Craton (NCC) constitutes China's largest gold province and one the major gold field in Asia (Goldfarb and Santosh, 2014) (Fig. 1). The gold mineralization formed at a short time scale around 125–120 Ma (Yang et al., 2000; Li et al., 2003; Li et al., 2006; Jiang et al., 2009; Goldfarb and Santosh, 2014; Song et al., 2015a; Fan et al., 2016), and has been universally classified into two types: (1) the Linglong-type, occurring as extensional massive gold-quartz-pyrite veins, is typically represented by the Linglong, Jiuqu, Jingqingding and Denggezhuang deposit; and (2) the Jiaojia-type, originally named from the Jiaojia deposit, occurs as disseminated veinlets and disseminated mineralization in wallrocks along fractures, including Sanshandao and Dongfeng deposits, except for the Jiaojia deposit (Fan et al., 2003, 2016; Song et al., 2012; Li et al., 2013; Li et al., 2015; Song et al., 2015a; Wen et al., 2015).

The origin of the gold deposits in the Jiaodong Peninsula is being debated, although numerous scientific studies have been carried out (e.g. Yang et al., 2000; Li et al., 2003; Zhai et al., 2004a; Li et al., 2006; Jiang et al., 2009; Zhai and Santosh, 2011; Goldfarb and Santosh, 2014; Song et al., 2015a; Fan et al., 2016; Jiang et al., 2016; Yang et al., 2016). There are two different viewpoints of the origin, orogenic and anorogenic. The former is based on structural settings and ore fluid geochemistry, mainly supported by Goldfarb et al. (2007); the latter is supported by other researchers who compared the tectonic setting and mineralization characteristics of Jiaodong deposits with those of typical orogenic gold deposits over the world, and pointed out that the gold deposits in Jiaodong Peninsula are distinct to the typical orogenic deposits, which are better to be named "Jiaodong-type" gold deposits (Zhai et al., 2004b), recently it was changed to "decratonic-type" gold deposits (Zhu et al., 2015). Most importantly, though, the characteristics of hydrothermal alteration and gold mineralization have been defined clearly, despite the debated origin.

Hydrothermal alteration process always commences from potassic alteration, through silicification and sericitization, to sulfidation, and ends at the carbonatization stage (Fig. 2). Potassic

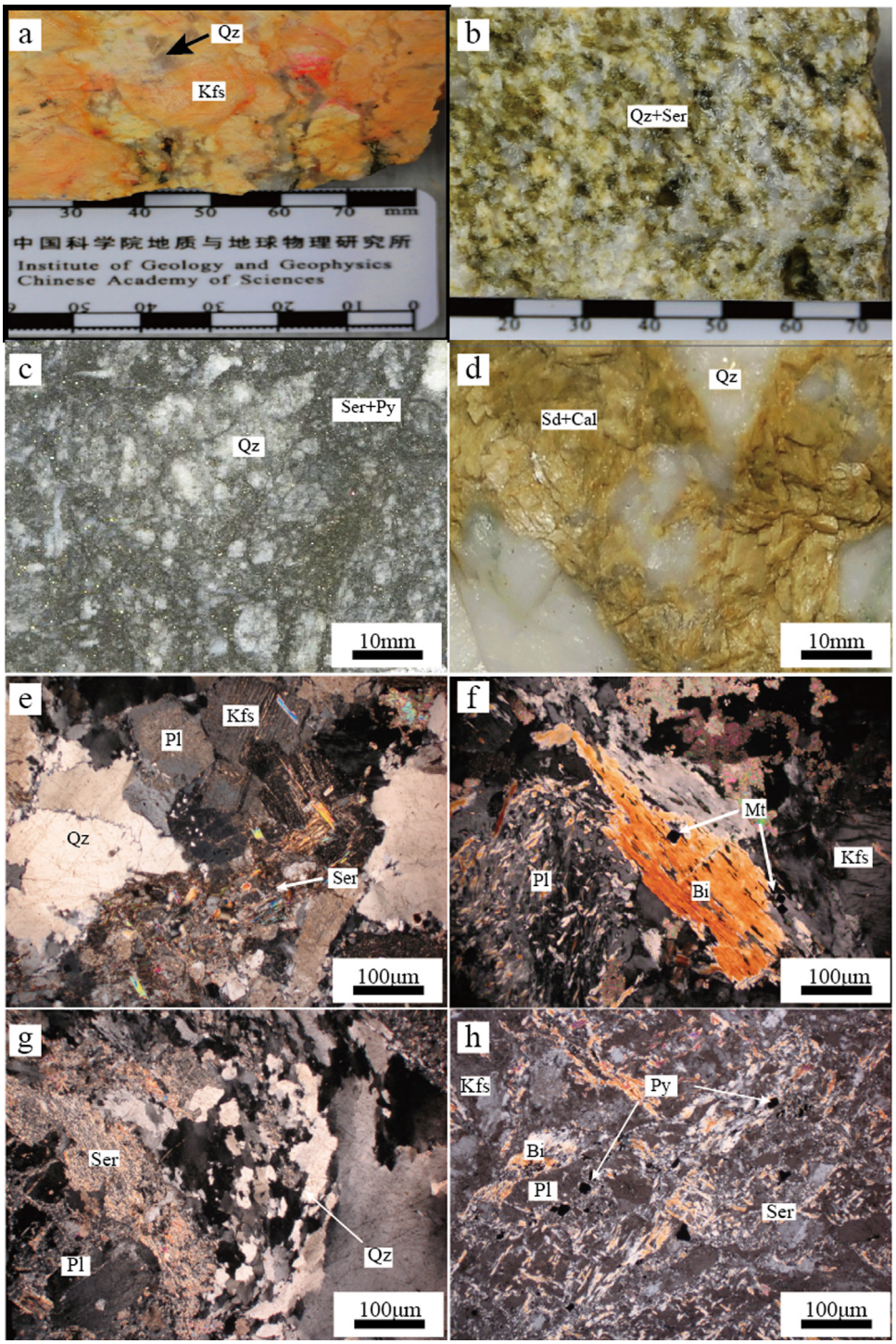

Fig. 2. Typical hydrothermal alteration of the Mesozoic granites in Jiaodong district. (a-d) photography in hand specimen, (e-h) transmitted light cross-polars photomicrographs.
(a,e,f) Potassic alteration, mainly composed of K-feldspar, quartz, and minor sericite and magnetite; (b,g) Sericitization, showing dark green color in hand specimen; (c,h) Sulfidation + sericitization, the main ore in this district with amount of gold-bearing pyrite; (d) Carbonatization, the last hydrothermal alteration stage with main minerals of calcite, siderite and quartz. Abbreviations: Bi = biotite, Cal = calcite, Kfs = K-feldspar, Mt = magnetite, Pl = plagioclase, Py = pyrite, Qz = quartz, Sd = siderite, Ser = sericite.

alteration is adjacent to fresh granite along brittle fractures in the granitic wall rocks, and is developed to a various degree in these deposits, with a thickness range of several meters to 50–60 m. The main alteration minerals are K-feldspar, quartz and sericite, with minor magnetite (Fig. 2a,e,f). Relic plagioclase is present in weakly altered rocks, and is partially transformed to sericite (Fig. 2e). Within the zone of the strong potassic alteration, the original igneous texture is obliterated, and pink secondary K-feldspars are dominant, replacing the magmatic plagioclase. The quartz proportion in the potassic alteration zone increases sharply inward, induced by silicification that followed the potassic alteration. Silicification includes quartz replacement of previous minerals and formation small quartz veins that always contain some amounts of sericite (Fig. 2b,g). Therefore, it is difficult to be distinguished

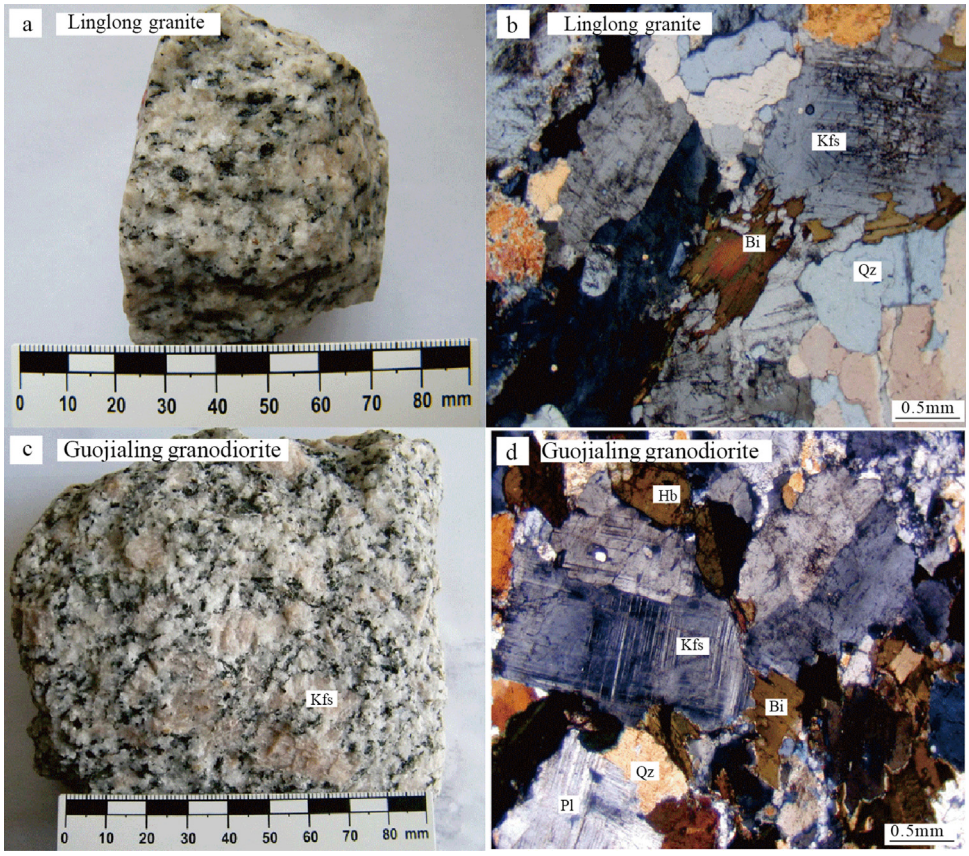

Fig. 3. Photography of Linglong granite and Guojialing granodiorite. Abbreviations same as above.

from the sericitization at hand specimen scale, except where the silicification is so strong that most silicate minerals are replaced by quartz with minor sericite and sulfide. As the proportion of sericite progressively increases, the silicification gradually gives way to sericitization. Sericitization, representing the most significant gold producing alteration zone, is black to dark green in color due to its high sulfide content (Fig. 2c). The primary rock is completely replaced by quartz, sericite and pyrite (Fig. 2h). Other alteration minerals, such as chlorite, epidote, and some minor sulfides including pyrrhotite, bornite, arsenopyrite and argentite, are also mentioned in some of the literature (e.g.; Li et al., 2015). Gold mineralization is temporally followed by carbonatization, the latest alteration in this district, which is mainly composed of calcite and siderite, always bordering the quartz veins (Fig. 2d).

All these hydrothermal alterations were acting on the chemical composition of granitic wall rocks, especially the widely distributed Linglong and Guojialing granitoids. The Jurassic Linglong granite (158–160 Ma) intruded into the TTG (Trondhjemite-Tonalite-Granodiorite) gneiss and amphibolites of the Late Archean Jiaodong Group, the main basement in Jiaodong district (Fig. 1). It is fine- to medium-grained, equigranular and mainly composed of plagioclase (25–30 vol.%), K-feldspar (35–40 vol.%), quartz (20–30 vol.%) and biotite (5–10 vol.%) (Fig. 3a,b). Previous studies revealed that the Linglong granite was mainly derived from partial melting of the ancient crust in the NCC (Miao et al., 1998; Hou et al., 2007). The 126–130 Ma Guojialing granodiorite is the main early Cretaceous intrusion in this district (Fig. 1), characterized by huge K-feldspar phenocrysts, with the largest crystals > 10 cm, showing porphyritic granite texture, and the main minerals are plagioclase (35–55%), K-feldspar (10–25%), quartz (15–30%), biotite (4–6%) (Fig. 3c,d). Geochemical and isotopic studies indicate that the Guojialing granodiorite was derived mainly from a crustal source, but with an involvement of mantle components (Yang et al., 2012). Vertically, the Linlong granite is mainly located at a shallow level, whereas the Guojialing granodiorite is always concealed at deeper levels. These Mesozoic intrusive rocks are extensively altered by hydrothermal fluid and contain disseminated gold-bearing sulfides, and will be treated as the main objects for the subsequent geochemical modeling.

3. Calculation methods and data sources

To evaluate the differences of gold mineralization efficiency in hydrothermal alteration processes of the Linglong and Guojialing granitoids, we have performed multicomponent fluid-rock equilibria geochemical modeling. All calculations were done with the GEM-Selektor Gibbs free energy minimization package (Kulik et al., 2013), which uses an interior point global optimization method to evaluate phase stability and speciation (Karpov et al., 1997; Kulik et al., 2013).

The thermodynamic dataset used for this geochemical modeling covers all main aqueous species and rock-forming minerals in the Si-Al-Fe-Mg-Ca-Na-K-Au-C-S-H-O-Cl system involved in this study. Data for charged and neutral aqueous species were compiled from Slop98 database in SUPCRT92 package developed and extended by Shock et al. (1992, 1997) based on modified Helgeson-Kirkham-Flowers (HKF) equation of state (Helgeson et al., 1981; Tanger and Helgeson, 1988). The data for rock-forming minerals and sulfides were taken from the internally consistent database of Holland and Powell (1998). Hauzenberger et al. (2002) and Pak et al. (2003) demonstrated that this dataset, in conjunction with the aqueous species data reviewed above, reproduces mineral solubility at elevated temperatures and pressures within their experimental uncertainty. Therefore, it is believed that the mineral and aqueous datasets are essentially self-consistent.

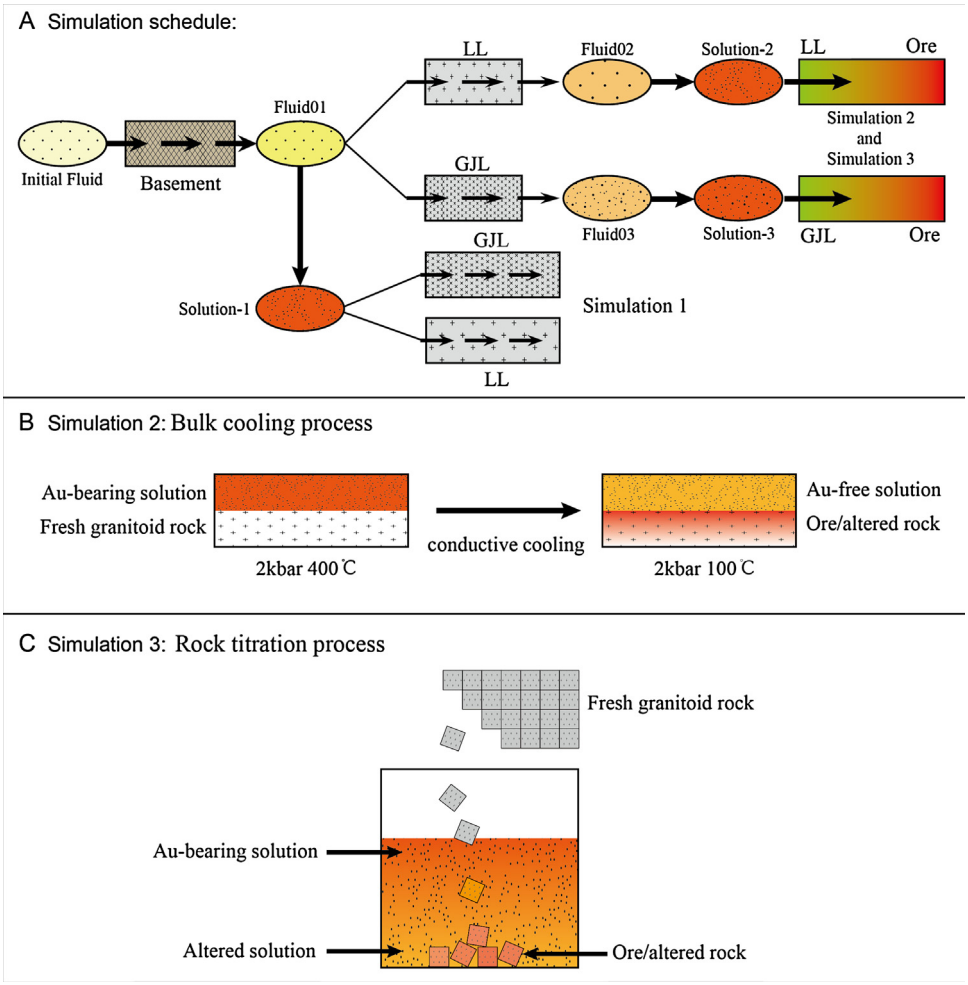

Fig. 4. Simulation schedule for geochemical modeling in this study. See construction in the text.

We have compiled the latest thermodynamic dataset for aqueous Au species, since these are the most important aqueous components in this study. Akinfiev and Zotov (2010) provided new HKF parameters for Au chloride, hydrosulfide and hydroxide complexes based on a review of existing experimental studies, the reliable temperature-pressure range is 0–600 °C and 1–3000 bar. Thus, in our geochemical modeling, the maximum temperature and pressure was set at 600 °C and 3000 bar, respectively.

Since the aqueous activity coefficients were calculated with the extended Debye-Hückel equation (Helgeson et al., 1981), the concentration of NaCl of the fluid should be lower than 4.5 mol/kg, in order to obtain accurate simulation results.

4. Geochemical simulations

Previous research revealed that the ore-forming fluids for gold mineralization in the Jiaodong district exhibit low salinity (0–8 wt.% NaCl equiv.), moderate temperature (ca. 250–300 °C) and pressure (1–2 kbar), with some content of CO_2 and minor CH_4 (Fan et al., 2003; Jiang et al., 2011; Hu et al., 2013; Wen et al., 2015). The concentration of Na, Cl, and C of the initial fluid was consistently set to 1 mol/kg water, simply calculated from the literature reviewed above, which was used to constrain the composition of the initial fluid. The other components were extremely dilute and will be calculated by fluid-mineral equilibria method, as described by Reed (1998).

Since the initial composition of the fluid was constrained, geochemical simulations were then designed based on the geologic settings in Jiaodong district (Fig. 4A). The initial fluid flows through the basement rock, i.e., TTG gneiss, paragneiss, and amphibolite, with their composition listed in Table 1. During this flow, the rock-forming elements in the fluid can be buffered by the rock and the concentrations of these elements are calculated hence. In this process, the temperature and pressure is fixed at 600 °C and 3 kbar, with rock mass of 1000 g. The resulting fluids are then cooled and depressurized to 500 °C and 2 kbar, producing Fluid01. For different basement rock, we named the samples as Fluid01-T, Fluid01-P, and Fluid01-A, corresponding to TTG gneiss, paragneiss, and amphibolite.

Gold concentration decreases as the ore-forming fluid flows through wall rocks, i.e. dilution process. Simulation 1 is specifically designed to evaluate the degree of gold dilution as the ore-forming fluid flows through the granitic wall rock. The Fluid01 produced above will become saturated with pyrite and gold here at fixed T-P condition, and finally turn to be Solution-1, with T, P, A subdivisions corresponding to Fluid01-T, Fluid01-P, and Fluid01-A, respectively (Table 2).

Simulations 2 and 3 are designed to model the gold precipitation process during hydrothermal alteration of the granitoids, in which the ore-forming fluids are also evolved from Fluid01. Because the major basement rock in Jiaodong district is the Archean TTG gneiss of the Jiaodong Group (Fig. 1) (Zhai et al., 2004a; Tang et al., 2007; Goldfarb and Santosh, 2014; Li et al., 2015; Song et al.,

Table 1
Chemical compositions of the basement and wall rocks (wt.%; TTG = Trondhjemite-Tonalite-Granodiorite, GJL = Guojialing granodiorite, LL = Linglong granite).

Rock	Sample	SiO_2	Al_2O_3	Fe_2O_3	FeO	MgO	CaO	Na_2O	K_2O	Total[c]
Basement[a]	TTG gneiss	73.39	14.93	0.17	1.13	0.55	2.79	4.03	1.68	98.67
	Para-gneiss[b]	66.39	14.33	0.61	5.75	2.89	2.17	1.98	1.85	95.97
	Amphibolite[b]	49.79	15.46	2.01	11.1	4.14	8.74	3.26	0.75	95.25
GJL	GJL-1	68.6	15.57	0.65	1.96	1.44	3.15	4.13	4.52	100.02
	GJL-2	67.89	15.32	0.57	2.15	1.53	3.22	4.36	4.45	99.49
	GJL-3	67.08	16.33	0.59	2.15	1.62	3.56	4.56	3.88	99.78
	GJL-4	66.59	15.77	0.62	1.85	1.31	3.06	4.16	3.36	96.72
	Av.	67.54	15.75	0.61	2.03	1.48	3.25	4.30	4.05	99.00
LL	LL-1	71.18	15.51	0.13	0.62	0.61	2.35	4.39	3.2	97.99
	LL-2	68.97	15.52	0.41	0.71	0.42	2.28	4.14	3.7	96.15
	LL-3	72.42	16.88	0.54	0.85	0.39	2.34	5.12	2.44	100.98
	LL-4	71.23	15.31	0.56	0.96	0.27	2.2	4.13	3.95	98.61
	LL-5	74.38	13.63	0.36	0.71	0.37	1.92	3.64	3.19	98.20
	Av.	71.64	15.37	0.34	0.77	0.41	2.22	4.28	3.30	98.33

[a] Data from Tang et al., 2007.
[b] The Fenzishan Group metasedimentary rock.
[c] Only those used in this study are listed.

Table 2
Molality of the independent compositions (ICom) of the fluids for water-rock interaction simulations (mol/kg water).

Icom	Initial Fluid	Solution-1			Solution-2		Solution-3	
		T	P	A	400 °C	300 °C	400 °C	300 °C
Al	–	1.33e-4	5.04e-4	1.60e-5	1.56e-6	3.28e-7	1.42e-6	7.02e-8
Au	–	1.27e-6	1.87e-6	4.64e-7	6.99e-8	8.62e-8	8.11e-8	8.52e-8
C	0.1000	0.1002	0.1001	0.1002	0.1063	0.1062	0.1063	0.1062
Ca	–	8.46e-4	6.96e-4	9.29e-4	0.0194	0.0194	0.0207	0.0207
Cl	1.000	1.0062	1.0141	1.0145	1.0067	1.0067	1.0071	1.0070
Fe	–	1.23e-4	2.23e-5	0.0055	0.0174	0.0124	0.0028	0.0012
K	–	0.1318	0.0617	0.0717	0.1063	0.1063	0.1092	0.1092
Mg	–	1.21e-6	1.73e-7	2.25e-5	1.85e-4	1.85e-4	3.94e-5	3.94e-5
Na	1.000	0.8956	1.0421	0.9312	0.8258	0.8258	0.8508	0.8508
ΣS	–	0.1657	0.1148	0.2371	0.0213	0.0186	0.0213	0.0181
Si	–	0.0914	0.1247	0.0804	0.0489	0.0238	0.0489	0.0238
pH		5.9	6.2	5.2	4.1	2.4	4.5	2.9
$lgfO_2$		−22.1	−24.2	−26.1	−27.5	−33.5	−27.3	−33.5

2015a), only the Fluid01-T is applied for subsequent simulations. Before testing gold mineralization process, the Fluid01 is allowed to flow through the granitoids under constant P-T conditions, producing Fluid02 and Fluid03 for Linglong and Guojialing granitoid, respectively. Since the ore-forming fluids are frequently slightly undersaturated with respect to their metal load, such as Au, Cu, before their arrival to the sites of ore precipitation (Audetat et al., 1998; Audetat et al., 2008; Rauchenstein-Martinek et al., 2014), the gold saturation degree of Fluid02 and Fluid03 should be tested. In this process, the tested fluids are cooled to 400 °C and 300 °C, respectively, with a constant pressure of 2 kbar. The cooled fluids are then supersaturated by gold, and because of the low sulfur concentration, the total amount of dissolved gold should be limited. Then, sulfur is added into the fluids until pyrite precipitates, and at this point it is believed that gold is saturated. For further simulations, the same gold concentration value is picked, both slightly undersaturated for Fluid02 and Fluid03, with different S contents. The gold-bearing fluids are labelled as Solution-2 and Solution-3 corresponding to Fluid02 and Fluid03, respectively, with their subdivisions of 400 °C and 300 °C (Table 2). After these procedures, Simulation 2 and 3 are then executed.

Simulation 2 is called "Bulk cooling" process, sequentially lowering the temperature to 100 °C at fixed bulk composition with a constant pressure (2 kbar) (Fig. 4B). This process is executed only for Solution 2 and 3 starting at 400 °C. Gold-bearing solution (1000 g) is placed into a box with 1000 g of fresh granitic rock inside, and water-rock interactions begin until equilibrium is reached. Then, the bulk system is cooled to 100 °C, generating a hydrothermally altered rock with gold and gold-poor solution. This simulation represents a static hydrothermal alteration process, modeling a fast fluid injection into a site where water-rock interaction took place and gold mineralization occurred.

Simulation 3 is a "Rock titration" process (Fig. 4c), introduced by Reed (1997, 1998). In this process, small fresh rock fragments are titrated into the gold-bearing solution one after the other; each addition changes the bulk composition of the water-rock system. After each titration increment, the system of equilibrium equations is solved to identify the equilibrium mineral assemblage and distribution of aqueous species. The 400 °C and 300 °C solutions are both evolved in this simulation, to investigate the hydrothermal alteration and gold precipitation processes at different temperatures. This simulation represents a slow injection of the ore-forming fluid into a fresh wall rock, and water-rock interactions take place step by step as the reacting fluid flows.

5. Results and discussions

5.1. Simulation 1: gold dilution modeling

When a gold-bearing solution flows through wall rocks, gold could be precipitated and dispersed in rocks, causing diminution of gold concentration in the primary solution. In order to test the gold precipitation capability of the Linglong and Guojialing intrusive rocks, Simulation 1 was executed.

The primary gold-bearing solutions were evolved from Fluid01-T, −P and −A, flowing through the basement rocks, TTG gneiss, paragneiss, and amphibolite, respectively. These rock types outcrop extensively in Jiaodong Peninsula. These solutions then passed

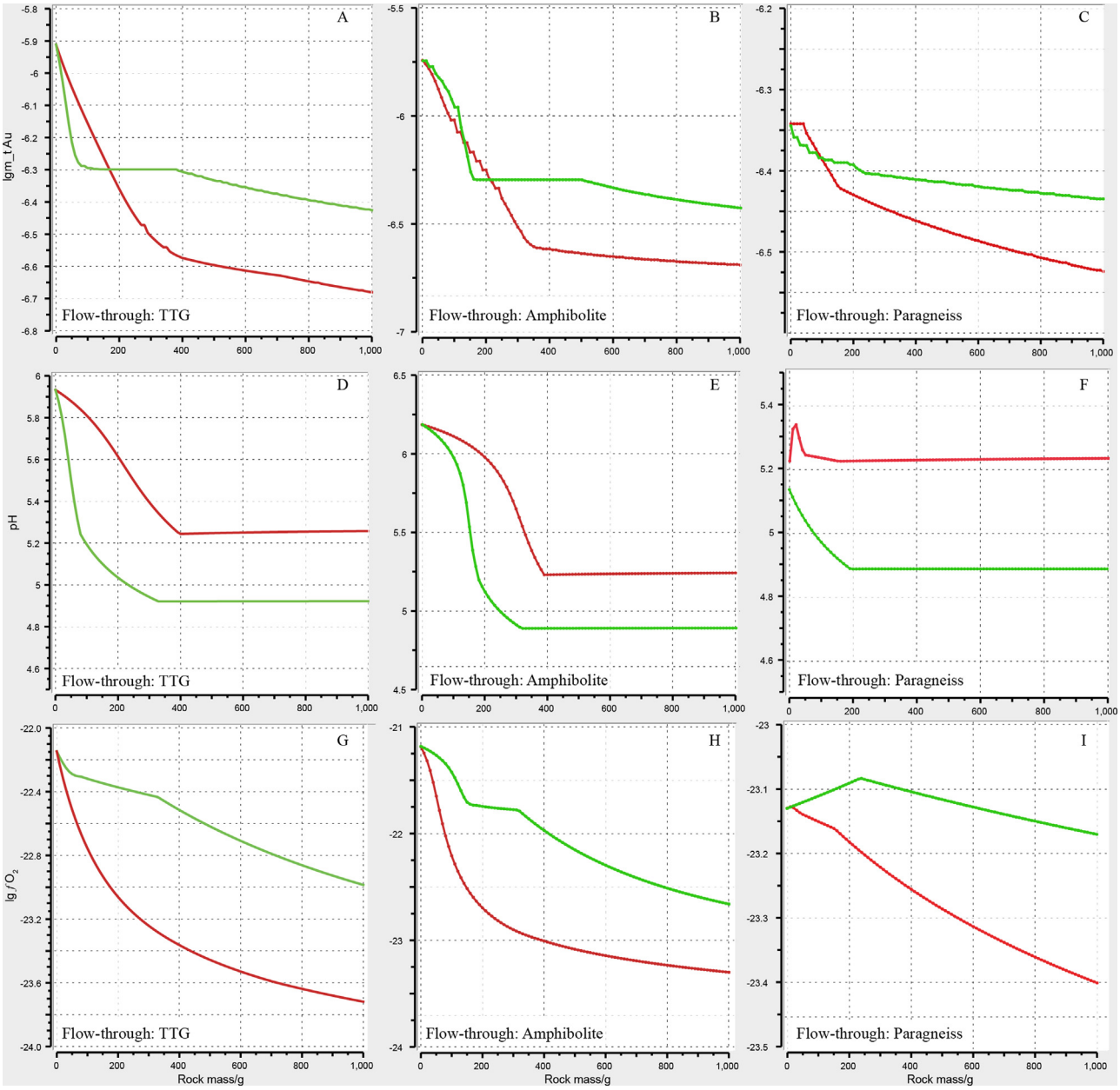

Fig. 5. Gold dilution modeling results of Simulation 1. The green and red line represents Linglong-solution and Guojialing-solution system, respectively. The ordinate of A-C presents total Au content in solution, and the abscissa is the rock mass flowed-through by the solution. (For interpretation of the references to colour in this figure legend, the reader is referred to the web version of this article.)

through the Linglong and Guojialing granitoids, and their gold concentration varied progressively as displayed in Fig. 5A-C, together with pH and oxygen fugacity changes (Fig. 5D-I). As solutions flowed through the rocks, their gold concentration decreased dramatically at first and then stabilized at low values. Comparatively, gold concentration in solutions flowing through the Linglong granite (green line in Fig. 5) is higher than that in solutions flowing through the Guojialing granodiorite (red line in Fig. 5), indicating that the gold precipitation ability of the Linglong granite is poorer than that of the Guojialing granodiorite. The pH and oxygen fugacity data were also monitored in this simulation. It is obvious that the Guojialing granodiorite can effectively buffer the pH of the solutions at a high level, whereas the pH value buffered by Linglong granite is relatively lower (Fig. 5 D-F). On the contrary, oxygen fugacity of the solutions flowing through the Linglong granite is higher (Fig. 5 G-I). Since the starting solution in each simulation sector is physicochemically the same, the only reason causing these differences is interaction with the wall rocks.

The iron content in these two different rocks is distinct, and the Guojialing granodiorite contains more Fe than the Linglong granite (Table 1). Fe oxides can effectively buffer the pH value of the reacted solution:

$$FeO + 2H^+ + Cl^- = FeCl^+ + H_2O$$

$$Fe_2O_3 + 6H^+ + 4Cl^- = 2FeCl_2^+ + 3H_2O$$

Therefore, the same quantity of Guojialing granodiorite consumes more H^+ than the Linglong granite does, and hence the pH value of the solutions buffered by the Guojialing granodiorite is higher than that by the Linglong granite. Besides, as revealed by some researchers, iron is the most effective precipitation agent for gold from its complexes (e.g. Arehart et al., 1993; Gammons and

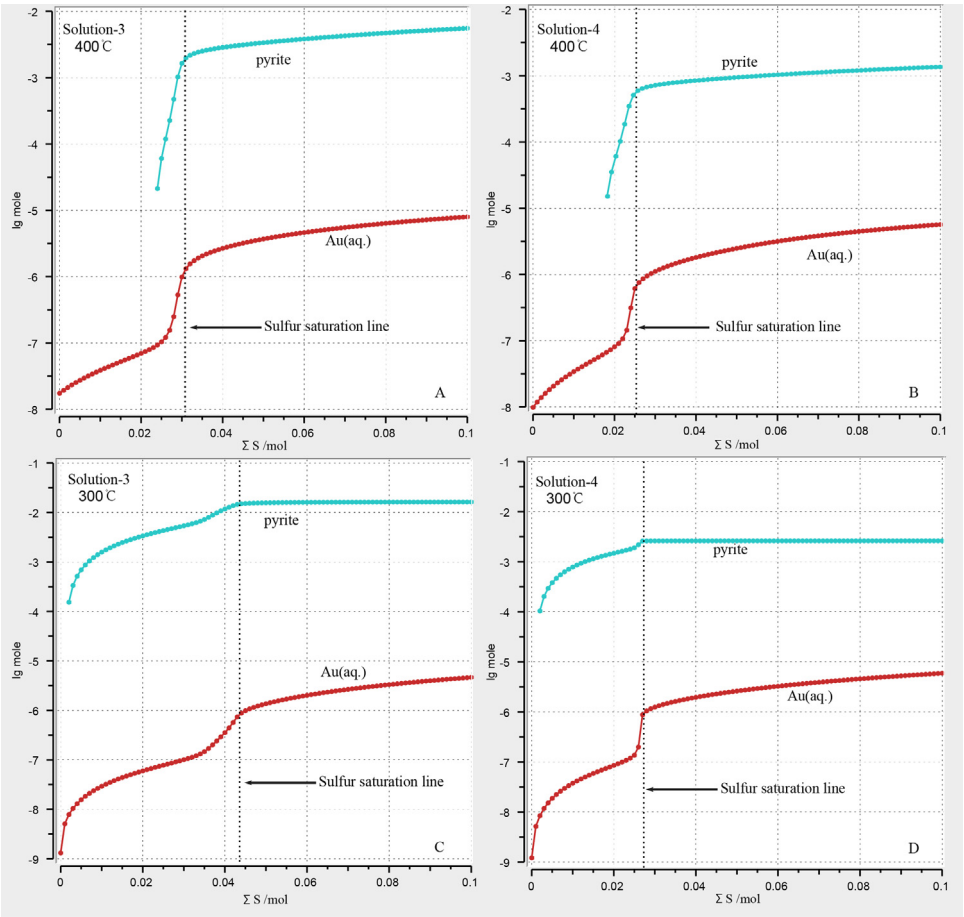

Fig. 6. Gold saturation testing results. Solution-3 is for Linglong granite, and Solution-4 is for Guojialing granodiorite. The ordinate is logarithm moles of pyrite precipitating from the solution and Au dissolved into the solution, and the abscissa is total sulfur mole titrating into the solution.

Williams-Jones, 1997; Williams et al., 2005; Williams-Jones et al., 2009; Richards, 2011):

$$FeCl^{+} + 2AuHS_{aq} = FeS_{2(py)} + 2Au^{0} + 2H^{+} + Cl^{-}$$

$$FeCl^{+} + 0.25O_{2,aq} + Au(HS)_2^{-} = FeS_{2(py)} + Au^{0} + H^{+} + Cl^{-} + 0.5H_2O$$

More $FeCl^{+}$ and less H^{+} will definitely enhance gold precipitation from the solution and lower the oxygen fugacity simultaneously.

Conclusively, the wallrock Guojialing granodiorite is less favorable for gold precipitation from the ore-forming fluid.

5.2. Gold saturation test

Gold solubility is controlled by many factors, such as temperature, pressure (especially that in vapor), concentration of ligands (such as S and Cl), pH, oxygen fugacity, and others (Benning and Seward, 1996; Gammons and Williams-Jones, 1997; Akinfiev and Zotov, 2001, 2010; Archibald et al., 2001; Stefánsson and Seward, 2003a, 2003b, 2004; Williams et al., 2005; Williams-Jones and Heinrich, 2005; Williams-Jones et al., 2009; Mei et al., 2014), and these parameters are frequently used to test the fertility of an ore-forming fluid.

For comparing the gold fertility of the solution in equilibrium with the rocks in interest, we executed a simulation testing gold saturation capacity. The point of pyrite precipitation is treated as gold saturation state, since gold is predominately hosted by pyrite. Simulation results show that both at high (400 °C) and low (300 °C) temperature, Solution03 in equilibrium with Linglong granite can accommodate more sulfur content than Solution04 that is in equilibrium with the Guojialing granodiorite (Fig. 6). The more sulfur content accommodated by Solution03 is probably attributed to its low Fe content. However, gold concentration in these two solutions at saturation point is comparatively similar with tiny difference (see Fig. 6). Accordingly, it is concluded that the fertility of the solutions flowing through the Linglong and Guojialing rocks is comparable.

5.3. Simulation 2: bulk cooling process

If gold mineralization took place in a fractured zone where an ore-forming fluid is injected and then steadily interacts with the granitoid rocks, "*Bulk cooling*" model then can be used to simulate this process. At the beginning, the starting solution interacted with fresh wall rock at 400 °C, until reaching an equilibrium state. Then temperature decreased, the resulting gold-bearing solution repeatedly interacted with the chemically changed wall rocks, keeping the bulk composition fixed.

Simulation results show that gold precipitation pattern is similar between the Linglong-Solution03 and Guojialing-Solution04 bulk system (Fig. 7), and gold was consistently precipitated from solution at ca. 350 °C and the precipitation peaked around 300 °C. However, the alteration mineral assemblages of these two bulk systems are partly different, especially with regard to sericite and magnetite (Fig. 8). Magnetite is locally developed in the Jiaodong district, and its total amount is low, which is inconsistent with the simulation result. We propose that magnetite is metastable in the sulfur-bearing hydrothermal fluids and is likely replaced by pyrite

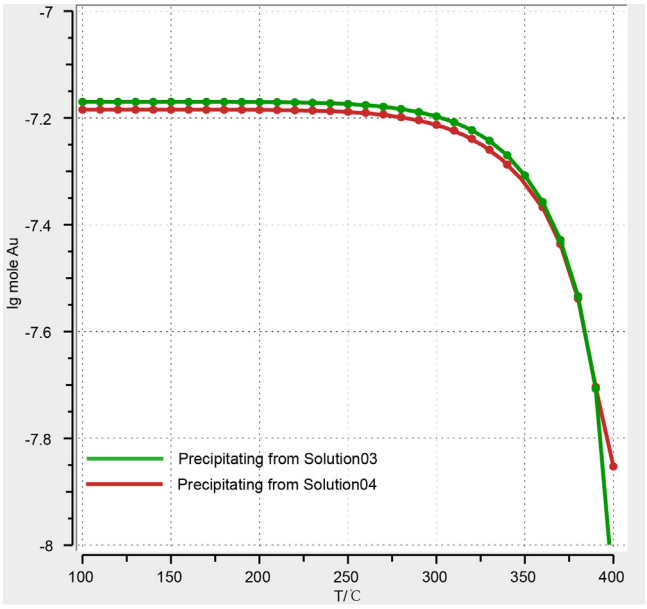

Fig. 7. Gold precipitation pattern in "Bulk cooling" process. The ordinate is logarithm mole of gold precipitating from solution, and the abscissa is temperature decreased from 400 °C to 100 °C.

or hematite (Sillitoe, 2003; Williams et al., 2005; Belperio et al., 2007; Tornos et al., 2010;). Sericite is predominant in hydrothermal alteration zones in this district, but according to the simulation results, sericite re-dissolved at temperatures lower than 150 °C in the Linglong-Solution03 system. Since the gold mineralization was formed in multiple stages, it is considered that the fixed system could be interrupted by later hot upwelling hydrothermal system, but it is far beyond our ability to simulate.

In summary, despite the chemical differences between the Linglong and Guojialing granitoids, their gold mineralization efficiency is probably similar, if the *Bulk cooling* process is the correct model.

5.4. Simulation 3: rock-titration process

Rock-titration model, also called "mass transfer", is most useful for studying hydrothermal alteration of wall rock along a fluid flow path, where it simulates the reactions responsible for forming the zoned alteration envelopes around the ore veins. As opposed to the *Bulk cooling* model, this model represents a fluid flow interacting with wall rock along its path. To investigate gold mineralization in this process at different temperatures, we executed two simulations at T = 400 °C and 300 °C, respectively.

5.4.1. Simulation at T = 400 °C

Titration of fresh wall rock into the solution resulted in progressive precipitation of gold. In the Linglong-Solution03 system, gold precipitation is prolonged. In the Guojialing-Solution04 system, gold steadily precipitated from the solution until the mass of the titrating rock reached 3000 g, and then no additional gold precipitated (Fig. 9A,B). The total gold mass in Guojialing case is slightly higher than that in Linglong case. Besides, based on a phase diagram of the alteration minerals (Fig. 9C,D), pyrite was only stable at the beginning, and was replaced by pyrrhotite as more of the rock was titrated into the solution, implying that gold is probably hosted by pyrrhotite rather than pyrite at high temperature. This is consistent with mineralogical and geochemical simulations in the Sanshandao gold deposit carried out by Xu et al. (2016).

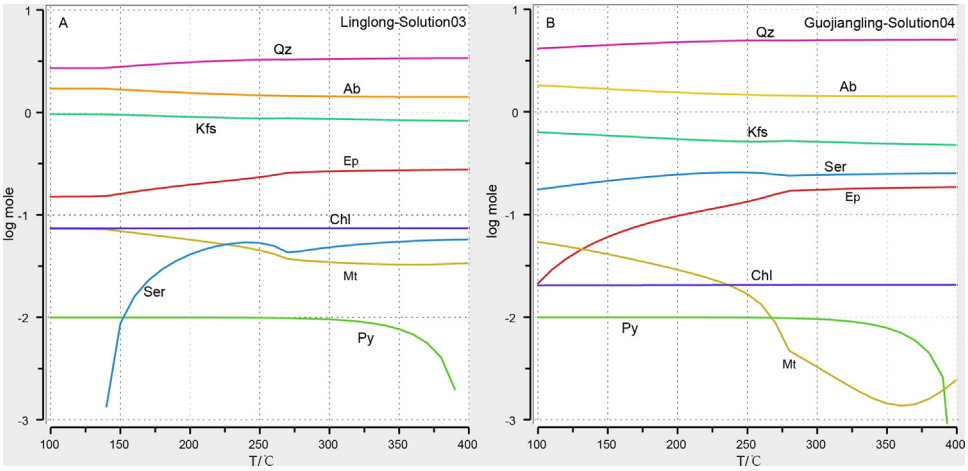

Fig. 8. Hydrothermal minerals precipitating from solution as temperature decreased. The ordinate is logarithm mole of minerals precipitating from solution, and the abscissa is temperature decreased from 400 °C to 100 °C.
Ab = albite, Chl = chlorite, Ep = epidotite, other abbreviations same as above.

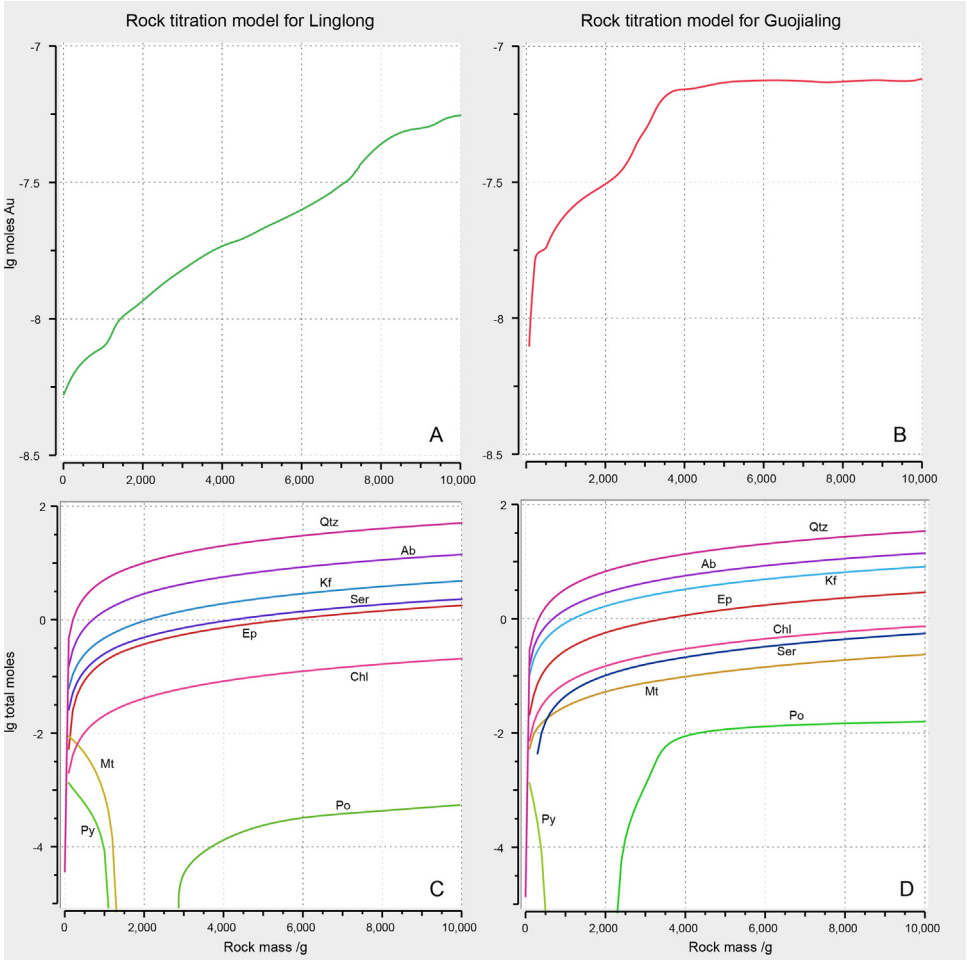

Fig. 9. Simulation results for "Rock-titration" process at T = 400 °C. The ordinate is logarithm mole of minerals precipitating from solution, and the abscissa is rock mass titrating into gold-bearing solution. Po = pyrrhotite, other abbreviations same as above.

Gold precipitation process is chemically described as:

$$FeO + AuHS^0 + 0.5H_{2,aq} = FeS_{(po)} + Au^0 + H_2O$$

Since the host mineral is pyrrhotite, and as mentioned above, the Guojialing can provide more FeO than the Linglong can in an unit rock mass. This is probably the reason causing their difference in gold mineralization efficiency.

The results indicate that the same quantity of gold precipitated from its parent solution altered less Guojialing granodiorite, which means the Guojialing granodiorite is more efficient for gold mineralization relative to the Linglong granite at high temperature, or equivalently at deep level, partly consistent with the deep prospecting results (unpublished mining reports).

5.4.2. Simulation at T = 300 °C

The simulation results are significantly different from those at 400 °C, in which gold mineralization efficiency of the Linglong case is higher than that of the Guojialing case, as shown in Fig. 10A,B. Rather than hosted by pyrrhotite at 400 °C, gold is precipitated with pyrite (Fig. 10.C,D). The exact reason leading to this difference is not clear and requires further work.

Numerous prospecting results show that gold is predominately associated with Linglong granite in shallow level (Fan et al., 2003; Li et al., 2015; Song et al., 2015a, 2015b). Since the temperature in the shallower levels is always lower than that in depth, the simulation results are well consistent with the prospecting observations.

6. Conclusions

The geochemical simulations in this study are based on the geologic background in the Jiaodong Peninsula, including lithology, mineralogy, and geochemistry. Hence, we consider that the research results are reliable in interpreting geological observations and guiding future prospecting and exploration.

According to the simulation results, in pathway of the gold-bearing solution, the wallrock Guojialing granodiorite is less favorable for gold precipitation from the ore-forming fluid. If the *Bulk cooling* process is the correct model, the gold mineralization efficiency of the Guojialing and Linglong granite is probably similar. However, in rock-titration process, the gold mineralization efficiency of the Guojialing and Linglong granite is different at various temperature conditions. The Guojialing granodiorite is prone to precipitate gold more strongly than the Linglong granite as gold-bearing solutions (or ore-forming fluids) flow through at higher temperature and greater depths. This implies that if the gold mineralization is developed at depth about, it prefers the Guojialing granodiorite; while if the gold-bearing solution flows through the wall rocks fast, and gold precipitation fails to take place, then the Guojialing granodiorite is probably unfavorable for subsequent gold enrichment of the ore-forming fluid. The Linglong granite is more efficient in gold precipitationfrom its parent solution at lower temperature and/or a shallower levels. Therefore, we suggest that the Guojialing granodiorite should be treated as the main target during the future deep prospecting project.

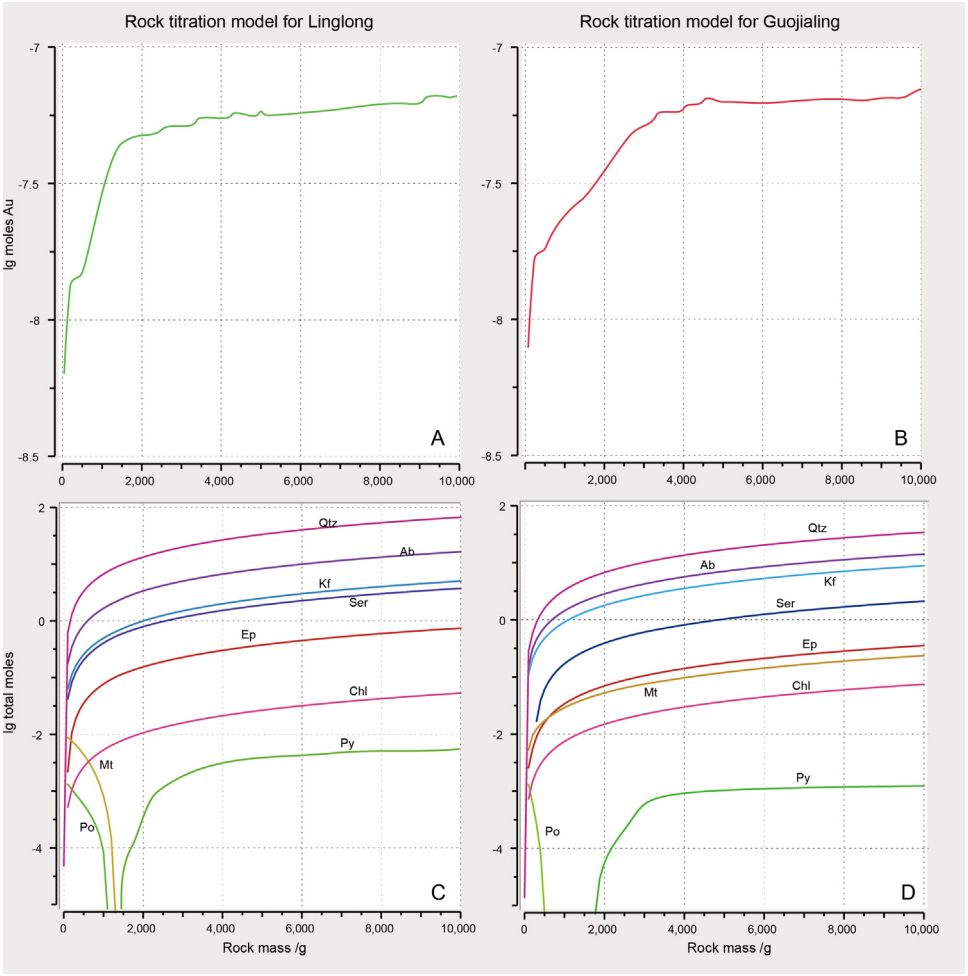

Fig. 10. Simulation results for "Rock-titration" process at T = 300 °C. The ordinate is logarithm mole of minerals precipitating from solution, and the abscissa is rock mass titrating into gold-bearing solution. Abbreviations same as above.

Acknowledgements

We gratefully acknowledge two anonymous referees, Associate Editor Dr. Juraj Majzlan and Editor-in-Chief Prof. Alex Deutsch for their constructive reviews and valuable comments which greatly contributed to the improvement of the manuscript. This study was financially supported by the National Natural Science Foundation of China (41502091 and 41672094) and Special Fund for Scientific Research in the Public Interest of Ministry of Land and Resources (No. 201411024-5).

References

Akinfiev, N., Zotov, A., 2001. Thermodynamic description of chloride, hydrosulfide, and hydroxo complexes of Ag (I), Cu (I), and Au (I) at temperatures of 25–500 °C and pressures of 1–2000 bar. Geochem. Int. 39 (10), 990–1006.

Akinfiev, N.N., Zotov, A.V., 2010. Thermodynamic description of aqueous species in the system Cu–Ag–Au–S–O–H at temperatures of 0–600 °C and pressures of 1–3000 bar. Geochem. Int. 48, 714–720.

Archibald, S.M., Migdisov, A.A., Williams-Jones, A.E., 2001. The stability of Au-chloride complexes in water vapor at elevated temperatures and pressures. Geochim. Cosmochim. Acta 65 (23), 4413–4423.

Arehart, G.B., Chryssoulis, S.L., Kesler, S.E., 1993. Gold and arsenic in iron sulfides from sediment-hosted disseminated gold deposits; implications for depositional processes. Econ. Geol. 88 (1), 171–185.

Audetat, A., Günther, D., Heinrich, C.A., 1998. Formation of a magmatic-hydrothermal ore deposit: insights with LA-ICP-MS analysis of fluid inclusions. Science 279 (5359), 2091.

Audetat, A., Pettke, T., Heinrich, C.A., Bodnar, R.J., 2008. The composition of magmatic-hydrothermal fluids in barren and mineralized intrusions. Econ. Geol. 103 (5), 877–908.

Belperio, A., Flint, R., Freeman, H., 2007. Prominent Hill: a hematite-dominated, iron oxide copper-gold system. Econ. Geol. 102 (8), 1499–1510.

Benning, L.G., Seward, T.M., 1996. Hydrosulphide complexing of Au (I) in hydrothermal solutions from 150 to 400 °C and 500–1500 bar. Geochim. Cosmochim. Acta 60 (11), 1849–1871.

Chen, Y.J., Pirajno, F., Qi, J.P., 2005. Origin of gold metallogeny and sources of ore-forming fluids, Jiaodong Province, Eastern China. Int. Geol. Rev. 47 (5), 530–549.

Fan, H.R., Zhai, M.G., Xie, Y.H., Yang, J.H., 2003. Ore-forming fluids associated with granite-hosted gold mineralization at the Sanshandao deposit, Jiaodong gold province, China. Miner. Deposita 38 (6), 739–750.

Fan, H.R., Feng, K., Li, X.H., Hu, F.F., Yang, K.F., 2016. Mesozoic gold mineralization in the Jiaodong and Korean peninsulas. Acta Petrologica Sinica 32, 3225–3238 (in Chinese with English abstract).

Gammons, C.H., Williams-Jones, A.E., 1997. Chemical mobility of gold in the porphyry-epithermal environment. Econ. Geol. 92 (1), 45–59.

Goldfarb, R.J., Santosh, M., 2014. The dilemma of the Jiaodong gold deposits: are they unique? Geosci. Front. 5, 139–153.

Goldfarb, R.J., Hart, C.J., Davis, G., Groves, D.I., 2007. East Asian gold—deciphering the anomaly of Phanerozoic gold in Precambrian cratons. Econ. Geol. 102, 341–346.

Hauzenberger, C.A., Baumgartner, L.P., Pak, T.T., 2002. Experimental study on the solubility of the model-pelite assemblage albite + K-feldspar + andalusite + quartz in supercritical chloride-rich aqueous solutions at 0.2 GPa and 600 °C. Geochim. Cosmochim. Acta 65, 4493–4507.

Helgeson, H.C., Kirkham, D.H., Flowers, G.C., 1981. Theoretical prediction of the thermodynamic behavior of aqueous electrolytes by high pressures and temperatures; IV, Calculation of activity coefficients, osmotic coefficients, and apparent molal and standard and relative partial molal properties to 600 °C and 5 kb. Am. J. Sci. 281 (10), 1249–1516.

Holland, T., Powell, R., 1998. An internally consistent thermodynamic data set for phases of petrological interest. J. Metamorph. Geol. 16 (3), 309–343.

Hou, M.L., Jiang, Y.H., Jiang, S.Y., Ling, H.F., Zhao, K.D., 2007. Contrasting origins of late Mesozoic adakitic granitoids from the northwestern Jiaodong Peninsula,

east China: implications for crustal thickening to delamination. Geol. Mag. 144 (04), 619–631.
Hu, F.F., Fan, H.R., Jiang, X.H., Li, X.C., Yang, K.F., Mernagh, T.P., 2013. Fluid inclusions at different depths in the Sanshandao gold deposit, Jiaodong Peninsula, China. Geofluids 13 (4), 528–541.
Jiang, S.Y., Dai, B.Z., Jiang, Y.H., Zhao, H.X., Hou, M.L., 2009. Jiaodong and Xiaoqinling: two orogenic gold provinces formed in different tectonic settings. Acta Petrol. Sin. 25 (11), 2727–2738 (in Chinese with English abstract).
Jiang, X.H., et al., 2011. Comparative studies on fluid inclusion in different depths and ore genesis of the Sanshandao gold deposit, Jiaodong Peninsula. Acta Petrol. Sin. 27 (5), 1327–1340 (in Chinese with English abstract).
Jiang, P., Yang, K.F., Fan, H.R., Liu, X., Cai, Y.C., Yang, Y.H., 2016. Titanite-scale insights into multi-stage magma mixing in early cretaceous of NW jiaodong terrain, north China craton. Lithos 258, 197–214.
Jiang, X.H., 2011. Ore-forming Fluid Evolution and Gold Mineralization of Alteration Type Gold Deposits in the Northwestern Jiaodong Peninsula. Doctor Degree Thesis. University of Chinese Academy of Sciences, Beijing, China, pp. 119 (in Chinese with English abstract).
Karpov, I.K., Chudnenko, K.V., Kulik, D.A., 1997. Modeling chemical mass transfer in geo- chemical processes: thermodynamic relations, conditions of equilibria, and numerical algorithms. Am. Jour. Sci. 297, 767–806.
Kulik, D.A., Wagner, T., Dmytrieva, S.V., Kosakowski, G., Hingerl, F.F., Chudnenko, K.V., Berner, U.R., 2013. GEM-Selektor geochemical modeling package: revised algorithm and GEMS3K numerical kernel for coupled simulation codes. Comput. Geosci. 17 (1), 1–24.
Li, J.W., Vasconcelos, P.M., Zhang, J., Zhou, M.F., Zhang, X.J., Yang, F.H., 2003. 40Ar/39Ar constraints on a temporal link between gold mineralization, magmatism, and continental margin transtension in the Jiaodong gold province, eastern China. J. Geol. 111 (6), 741–751.
Li, J.W., Paulo, V., Zhou, M.F., Zhao, X.F., Ma, C.Q., 2006. Geochronology of the Pengjiakuang and Rushan gold deposits, eastern Jiaodong gold province, northeastern China: implications for regional mineralization and geodynamic setting. Econ. Geol. 101 (5), 1023–1038.
Li, X.C., Fan, H.R., Santosh, M., Hu, F.F., Yang, K.F., Lan, T.G., 2013. Hydrothermal alteration associated with Mesozoic granite-hosted gold mineralization at the Sanshandao deposit, Jiaodong gold province, China. Ore Geol. Rev. 53, 403–421.
Li, L., Santosh, M., Li, S.R., 2015. The 'Jiaodong type' gold deposits: characteristics, origin and prospecting. Ore Geol. Rev. 65 (Part 3), 589–611.
Mei, Y., Liu, W., Sherman, D.M., Brugger, J., 2014. Metal complexation and ion hydration in low density hydrothermal fluids: ab initio molecular dynamics simulation of Cu(I) and Au(I) in chloride solutions (25–1000 °C, 1–5000 bar). Geochim. Cosmochim. Acta 131 (0), 196–212.
Miao, L., Luo, Z., Guan, K., Huang, J., 1998. The implication of the SHRIMP U-Pb age in zircon to the petrogenesis of the Linglong granite, East Shandong Province. Acta Petrol. Sin. 14 (2), 198–206 (in Chinese with English abstract).
Pak, T.M., Hauzenberger, C.A., Baumgartner, L.P., 2003. Solubility of the assemblage albite+ K-feldspar + andalusite + quartz in supercritical aqueous chloride solutions at 650 °C and 2 kbar. Chem. Geol. 200, 377–393.
Rauchenstein-Martinek, K., Wagner, T., Wälle, M., Heinrich, C., 2014. Gold concentrations in metamorphic fluids: a LA-ICPMS study of fluid inclusions from the Alpine orogenic belt. Chem. Geol. 385, 70–83.
Reed, M., 1997. Hydrothermal Alteration and Its Relationship to Ore Fluid Composition. Geochemistry of Hydrothermal Ore Deposits. John Wiley & Sons, New York.
Reed, M., 1998. Calculation of simultaneous chemical equilibria in aqueous-mineral-gas systems and its application to modeling hydrothermal processes. Tech. Hydrothermal Ore Deposits Geol. 10, 109–124 (pp).
Richards, J.P., 2011. Magmatic to hydrothermal metal fluxes in convergent and collided margins. Ore Geol. Rev. 40 (1), 1–26.
Shock, E.L., Oelkers, E.H., Johnson, J.W., Sverjensky, D.A., Helgeson, H.C., 1992. Calculation of the thermodynamic properties of aqueous species at high pressures and temperatures. Effective electrostatic radii, dissociation constants and standard partial molal properties to 1000 °C and 5 kbar. J. Chem. Soc. Faraday Trans. 88 (6), 803–826.
Shock, E.L., Sassani, D.C., Willis, M., Sverjensky, D.A., 1997. Inorganic species in geologic fluids: correlations among standard molal thermodynamic properties of aqueous ions and hydroxide complexes. Geochim. Cosmochim. Acta 61 (5), 907–950.
Sillitoe, R., 2003. Iron oxide-copper-gold deposits: an Andean view. Miner. Deposita 38 (7), 787–812.
Song, M.C., Yi, P.H., Xu, J.X., Cui, S.X., Shen, K., Jiang, H.L., 2012. A step metallogenetic model for gold deposits in the northwestern Shandong Peninsula, China. Sci. China Earth Sci. 55 (6), 940–948 (in Chinese with English abstract).
Song, M.C., Li, S.Z., Santosh, M., Zhao, S.J., Yu, S., Yi, P.H., 2015a. Types, characteristics and metallogenesis of gold deposits in the Jiaodong Peninsula, Eastern North China Craton. Ore Geol. Rev. 65 (Part 3), 612–625.
Song, M.C., Zhang, J.J., Zhang, P.J., Yang, L.Q., 2015b. Discovery and tectonic-magmatic background of superlarge gold deposit in offshore of Northern Sanshandao, Shandong Peninsula, China. Acta Geol. Sin. 89 (2), 365–383.
Stefánsson, A., Seward, T.M., 2003a. The hydrolysis of gold(I) in aqueous solutions to 600 °C and 1500 bar. Geochim. Cosmochim. Acta 67 (9), 1677–1688.
Stefánsson, A., Seward, T.M., 2003b. Stability of chloridogold(I) complexes in aqueous solutions from 300 to 600 °C and from 500 to 1800 bar. Geochim. Cosmochim. Acta 67 (23), 4559–4576.
Stefánsson, A., Seward, T.M., 2004. Gold(I) complexing in aqueous sulphide solutions to 500 °C at 500 bar. Geochim. Cosmochim. Acta 68 (20), 4121–4143.
Tang, J., Zheng, Y.F., Wu, Y.B., Gong, B., Liu, X.M., 2007. Geochronology and geochemistry of metamorphic rocks in the Jiaobei terrane: constraints on its tectonic affinity in the Sulu Orogen. Precambrian Res. 152, 48–82.
Tanger, J.C., Helgeson, H.C., 1988. Calculation of the thermodynamic and transport properties of aqueous species at high pressures and temperatures; revised equations of state for the standard partial molal properties of ions and electrolytes. Am. J. Sci. 288 (1), 19–98.
Tornos, F., Velasco, F., Barra, F., Morata, D., 2010. The Tropezón Cu–Mo–(Au) deposit Northern Chile: the missing link between IOCG and porphyry copper systems? Miner. Deposita 45 (4), 313–321.
Wen, B.J., Fan, H.R., Santosh, M., Hu, F.F., Pirajno, F., Yang, K.F., 2015. Genesis of two different types of gold mineralization in the Linglong gold field, China: constrains from geology, fluid inclusions and stable isotope. Ore Geol. Rev. 65, 643–658.
Williams, P.J., Barton, M.D., Johnson, D.A., Fontbote, L., 2005. Iron oxide copper-gold deposits: geology, space-time distribution, and possible modes of origin. Econ. Geol., 371–405.
Williams-Jones, A.E., Heinrich, C.A., 2005. 100th Anniversary Special Paper: vapor transport of metals and the formation of magmatic-hydrothermal ore deposits. Econ. Geol. 100 (7), 1287–1312.
Williams-Jones, A.E., Bowell, R.J., Migdisov, A.A., 2009. Gold in solution. Elements 5 (5), 281–287.
Xu, W.G., Fan, H.R., Yang, K.F., Hu, F.F., Cai, Y.C., Wen, B.J., 2016. Exhaustive gold mineralizing processes of the Sanshandao gold deposit, Jiaodong Peninsula, eastern China: displayed by hydrothermal alteration modeling. J. Aisan Earth Sci. 129, 152–169.
Yang, J.H., Zhou, X.H., Chen, L.H., 2000. Dating of gold mineralization for super-large altered tectonite-type gold deposits in Northwestern Jiaodong Peninsula and its implications for gold metallogeny. Acta Petrol. Sin. 16 (3), 454–458 (in Chinese with English abstract).
Yang, Q.L., Zhao, Z.F., Zheng, Y.F., 2012. Modification of subcontinental lithospheric mantle above continental subduction zone: constraints from geochemistry of Mesozoic gabbroic rocks in southeastern North China. Lithos 146, 164–182.
Yang, L.Q., Deng, J., Wang, Z.L., Zhang, L., Goldfarb, R.J., Yuan, W.M., Weinberg, R.F., Zhang, R.Z., :surname>WangL.ZhangR.J.GoldfarbW.M.Yuan R.F.WeinbergR.Z.ZhangThermochronologic constraints on evolution of the Linglong Metamorphic Core Complex and implications for gold mineralization: a case study from the Xiadian gold deposit, Jiaodong Peninsula, eastern ChinaOre Geol. Rev.722016. Thermochronologic constraints on evolution of the Linglong Metamorphic Core Complex and implications for gold mineralization: a case study from the Xiadian gold deposit, Jiaodong Peninsula, eastern China. Ore Geol. Rev. 72, 165–178.
Zhai, M.G., Santosh, M., 2011. The early Precambrian odyssey of the North China Craton: a synoptic overview. Gondwana Res. 20 (1), 6–25.
Zhai, M.G., Fan, H.R., Yang, J.H., Miao, L., 2004a. Large-scale cluster of gold deposits in east Shandong: anorogenic metallogenesis. Earth Sci. Front. 11 (1), 85–98 (in Chinese with English abstract).
Zhai, M.G., Meng, Q.R., Liu, J.M., Hou, Q.L., 2004b. Geological features of Mesozoic tectonic regime inversion in Eastern North China and implication for geodynamics. Earth Sci. Front. 11, 285–294 (in Chinese with English abstract).
Zhu, R.X., Fan, H.R., Li, J.W., Meng, Q.R., Li, S.R., Zeng, Q.D., 2015. Decratonic gold deposits. Sci. China. Ser. D Earth Sci. 58, 1523–1537.